A TWO-DIMENSIONAL CELLULAR AUTOMATA MODEL OF

ABRASIVE WATER JET CUTTING

H. Orbanic and M. Junkar
Laboratory for Alternative Technologies, University of Ljubljana
Ljubljana, Slovenia

ABSTRACT

In this paper a new approach to modelling abrasive water jet (AWJ) cutting is presented. A cellular automata (CA) model was developed, which calculates the shape of the cutting front, which can be used as an estimation of the surface quality. The CA calculates the form of the cutting front by using the developed rules for material removal and propagation of AWJ. The model also generates a well-known step on the cutting front. The modelling with CA provides a visual narrative of the moving cutting front, which is impossible to observe in the cutting of opaque materials.

1. INTRODUCTION

Abrasive water jet (AWJ) machining is a non-conventional process, which uses high-velocity water jet to accelerate very hard abrasive grains. Because of their high velocity and hardness the grains remove material at impact with the workpiece. This type of machining belongs to solid particle erosion processes. The material removal rate depends on the kinetic energy of abrasive grains, their impact angles, eroded material type and type of abrasive grains (Levy, 1995). Following this assumption, Lebar and Junkar (2004) developed the unit event. The model studies the impact of each individual abrasive grain (unit event) and gives a cumulative result of all impacts in the form of machined surface topography. Other attempts to model AWJ machined surface topography were also made. Fukunishi et al. (1995, 1997) numerically simulated AWJ cut surface topography. Their work made use of Bitter's theory (Bitter, 1963) on erosion processes for predicting the striations on the cut surface. Vikram and Babu (2002) tried a similar approach. They also used Bitter's theory for predicting material removal and the theory of ballistics for predicting the trajectory of jet penetration into the material. In their simulation they obtained both striations and jet lag. Then they employed surface generation theory in order to generate surface topography. Yong and Kovacevic (1996) developed a numerical model for AWJ machining that includes several elements of the process, such as the simulation of multiphase pipe-flow, tracer record of abrasive particles and energy transformation in a defined material "memory cell". The workpiece surface area is divided into network of cells. After the kinematics of abrasive grains is calculated, each cell records the number of abrasive particles striking a small area of workpiece in order to predict the depth of cut at the point where the particular cell is situated. The joint result of all memory cells gives the resulting surface of the cut. Ditzinger et al. (1999) have studied non-linear dynamics of AWJ. They derived a partial differential equation, which describes the development of cutting front in time.

In this paper a new approach to modelling AWJ machining by using cellular automata (CA) is presented. CA were first introduced by John von Neumann in year 1950 (von Neumann, 1966). They have been widely used for modelling complex systems (Wolfram, 1994, Chopard, 1998). CA are convenient when the modelled process is difficult to describe mathematically but on the other hand there exist a lot of phenomenological knowledge about the process itself. The knowledge can include our own experience about the process, which was gathered through performing experiments or from literature. Because solid particle erosion is a very complex process, which is difficult to model (Levy, 1995), the CA could provide a better result. The modelling of erosion by using CA can be found in geology, where land erosion was studied (d'Ambrosio, 2001). This approach has not been previously used for modelling AWJ cutting but has been used to describe other types of material removal. One example is simulation of photoresist etching (Karafyllidis, 1995, 1999).

The algorithm was written for two-dimensional (2D) AWJ cutting process and will be in future expanded into third dimension. The CA algorithm models the AWJ cutting process on a mesoscopic level and was found to be fast because of lower complexity. The CA models the material removal process by considering the energy of AWJ together with its impact angle and erosion resistance of workpiece material. Another parameter, which significantly influences the shape of cutting front, is the cutting velocity or the traverse velocity of the jet. It determines how long AWJ will have an influence on a part of workpiece material. The lower the velocity, more material will be removed and the smaller is the curvature of the

cutting front. The step formation in CA model is based on the findings of Hashish (1988) and Guo (1993), which relate to the time interval of step formation and how the step influences the cutting process.

2. THE CA THEORY

CA represents an idealization of physical system, in which space and time are discrete, and the physical quantities take only a finite set of values (Chopard, 1998). They consist of equally distributed *d*-dimensional array, which can be of unlimited range. Each element of the array is characterized by a value of certain physical quantity. This physical quantity as a collection of all states in cells at certain time represents a global state of CA. On the other hand the value of the physical quantity in each cell represents a local state of CA. Each cell in CA can only interact with those cells, which are in its neighbourhood. An example of von Neumann type neighbourhood is shown in Figure 1, which was also used in the model described in this paper. As a consequence the cells in CA are not able to globally communicate with other cells (Wolfram, 1994). The neighbourhood is usually defined as the cell itself and the cells adjacent to it. In theory it could be of arbitrary shape and size but this would increase the complexity of CA. State of all cells is updated simultaneously in discrete time steps with regard to the state in their neighbouring cells in previous time step. Algorithm with which new states in cells are calculated is called a local rule of CA. Usually this rule is the same for all cells (Karafyllidis, 1995).

3. THE CA MODEL

The space, where AWJ cutting process takes place, is divided into an array of equally sized square cells. Three local states of CA cells are defined, which correlate to three areas found in the case of AWJ cutting. The particular cell can be in one of the three states: an empty space (ES), a state of abrasive water jet (AWJ) and a state of workpiece material (MAT). These three areas are schematically shown in Figure 2.

The ES state represents an empty cell and has a trivial role in CA. The AWJ state represents the intensity of the jet or its ability to remove material. The parameter of AWJ intensity *A* was introduced, which is connected to kinetic energy and depends on setup parameters of AWJ such as water pressure, water mass flow rate, abrasive mass flow rate, type and size of abrasive grains and geometry of the cutting head. Because of the complexity of AWJ forming process and high velocities the direct connection between listed parameters and kinetic energy is still part of the research and is currently not revealed yet. Once the connection is revealed its inclusion in CA is easy to implement.

The MAT state does not represent a quantity of material and is therefore defined by a removal resistance parameter *M*. The greater the value of parameter *M* the more time will be needed to remove a whole cell. The resistance is defined regarding the machinability number N_m as

$$M = \frac{10000}{N_m} \qquad (1)$$

The machinability number N_m was introduced by Zeng and Kim (1995). In their semi-empirical model for cutting with AWJ, N_m represents the unique property of the material under the condition of AWJ machining. It is an approximation of inverse machinability parameter of erosion resistance defined in theoretical model for calculating the depth of cut by the same authors. Because the theoretical model did not correlate well with experimental data they modified the theoretical model into a semi-empirical one. This model is a regression equation in which one of the parameters is also N_m. To calculate it the equation requires a large number of AWJ kerf cutting tests for different parameters and materials.

In order to describe the AWJ machining process, the developed CA model consists of two main parts and one auxiliary part. The first part calculates the material removal and the second one calculates the propagation of AWJ intensity. The third part checks the inclination of the cutting front at certain time intervals and induces the step formation process. After the initial values for parameters of AWJ A, M and cutting velocity are entered into the CA model the material removal step is performed. Then the propagation of AWJ intensity step is performed and temporary shape of the cutting front is obtained. The procedure, which is performed cyclically while the jet is moving with predetermined cutting velocity, is shown in Figure 3.

The material removal is performed when a neighbourhood cell of material cell contains AWJ state. Simultaneously the cell with AWJ state loses some of its energy, which was spent on removal. When the material cell is emptied it is replaced by cell state AWJ, which can then further influence other material cells, which were previously out of reach.

Additionally two coefficients of material removal were defined by considering the shape of the CA array and the neighbourhood shape. The chosen neighbourhood is von Neumann's and is composed of a cell itself and four adjacent cells (Figure 1). The first coefficient R_v is for vertical removal and the second one R_h is for horizontal removal, depending on the direction of AWJ propagation. The coefficients determine how much energy will be spent on material removal and how much the material resistance will be reduced. The important issue is determining the value of coefficients and their ratio. It can be concluded from visual observations of the AWJ cutting process (Hashish, 1988) that significantly more material is removed in vertical direction than in horizontal direction. Therefore the value of R_v will be several times higher than the one of the R_h. Lebar and Junkar (2003) performed a research on aluminium AL 6061-T6, where the mass of removed material depending on the impact angle of AWJ was measured. The results showed that the mass of removed material at impact angles under 20° is much smaller than at angles over 20°. According to these findings the coefficients of material removal can also be linked to the influence of the impact angle of AWJ on material removal. The two coefficients are multiplied with AWJ intensity parameter A in neighbouring cells as shown in equation (2) for calculating M in cell with coordinates i and j:

$$M_{i,j}^{t+1} = M_{i,j}^{t} - R_v \cdot \left(A_{i-1,j}^{t} + A_{i+1,j}^{t} \right) - R_h \cdot \left(A_{i,j-1}^{t} + A_{i,j+1}^{t} \right), \tag{2}$$

where $M_{i,j}^{t+1}$ is the material resistance at time step $t + 1$, $M_{i,j}^{t}$ the material resistance at time step t, and $A_{i-1,j}^{t}$, $A_{i+1,j}^{t}$, $A_{i,j-1}^{t}$, $A_{i,j+1}^{t}$ the AWJ intensities in the neighbourhood cells at time step t.

The R_v is considered in CA when AWJ state is in upper or lower cell of material cell, while the R_h is considered when AWJ state is in left or right cell of material cell. Usually the AWJ state is in the top and left cell if the jet is moving to the right. After the material removal calculations for the *(i,j)* cell are performed, the reduction of the AWJ intensity values in neighbouring cells is performed as shown in equations (3) to (6)

$$A_{i-1,j}^{t+1} = \text{sgn}\left(A_{i-1,j}^{t}\right) \cdot A_{i-1,j}^{t} \cdot (1 - R_v), \tag{3}$$

$$A_{i+1,j}^{t+1} = \text{sgn}\left(A_{i+1,j}^{t}\right) \cdot A_{i+1,j}^{t} \cdot (1 - R_v), \tag{4}$$

$$A_{i,j-1}^{t+1} = \text{sgn}\left(A_{i,j-1}^{t}\right) \cdot A_{i,j-1}^{t} \cdot (1 - R_h), \tag{5}$$

$$A_{i,j+1}^{t+1} = \text{sgn}\left(A_{i,j+1}^{t}\right) \cdot A_{i,j+1}^{t} \cdot (1 - R_h), \tag{6}$$

where $A_{i-1,j}^{t+1}$, $A_{i+1,j}^{t+1}$, $A_{i,j-1}^{t+1}$, $A_{i,j+1}^{t+1}$ are the AWJ intensities in neighbouring cells at the time step $t + 1$ and sgn*(x)* is the signum function of *x*, being +1 if $x > 0$, 0 if $x = 0$ and -1 if $x < 0$. By using the signum function, only cells which have AWJ state in the neighbourhood are included in the calculations.

The process of propagation of AWJ intensity gives a simplified version of jet flow in form of changing the jet intensity during its flow past the cutting front. Because this type of flow is complex and the jet has high kinetic energy as a consequence of high velocity, the jet is treated through its energy state or intensity. The jet was divided into cells, each with its own intensity. The flow is considered to be infinite and the intensity changes itself accordingly to the intensity state of their neighbouring cells and accordingly to spent energy for material removal. After the material removal step is performed, the values of AWJ intensity in cells with AWJ state are redistributed. The redistribution in the *(i,j)* cell is achieved by using the following weighted average of AWJ intensity values in all neighbouring cells with AWJ state:

$$
\begin{aligned}
A_{i,j}^{t+1} = &\left[w_1 \cdot A_{i-1,j}^{t} \cdot \text{sgn}\left(A_{i-1,j}^{t}\right) + w_2 \cdot A_{i,j-1}^{t} \cdot \text{sgn}\left(A_{i,j-1}^{t}\right) + w_3 \cdot A_{i,j}^{t} \cdot \text{sgn}\left(A_{i,j}^{t}\right) \right. \\
&\left. + w_4 \cdot A_{i,j+1}^{t} \cdot \text{sgn}\left(A_{i,j+1}^{t}\right) + w_5 \cdot A_{i+1,j}^{t} \cdot \text{sgn}\left(A_{i+1,j}^{t}\right) \right] \\
&\cdot \left[w_1 \cdot \text{sgn}\left(A_{i-1,j}^{t}\right) + w_2 \cdot \text{sgn}\left(A_{i,j-1}^{t}\right) + w_3 \cdot \text{sgn}\left(A_{i,j}^{t}\right) + w_4 \cdot \text{sgn}\left(A_{i,j+1}^{t}\right) + w_5 \cdot \text{sgn}\left(A_{i+1,j}^{t}\right) \right]^{-1},
\end{aligned} \tag{7}
$$

where w_1 to w_5 are weights used in calculating the average value. Because the distribution of AWJ intensity substitutes the flow of the jet from up to down, the weights are chosen in such manner that the upper cell in the neighbourhood has the largest weight. By using the signum function in equation (7) only cells, which have AWJ state in the neighbourhood, are included in the calculations.

The point where AWJ enters the area of CA or AWJ source is represented by a subarray of cells **S** in the first row of CA. The size of **S** corresponds to the width of the jet. The cells in the source have an initial value of AWJ intensity, which is then passed to the CA, when propagation step is performed. By entering the velocity with which the AWJ source is moving in the first row, the cutting velocity is defined. The setting of the cutting velocity is

implemented by using the floor function. The floor function $\lfloor x \rfloor$ gives the largest integer less than or equal to x. The function was included into main loop of CA in form of

$$\lfloor x \rfloor = \left\lfloor \frac{t}{t_c} \right\rfloor, \tag{8}$$

where t is a time step and t_c is a shifting coefficient, which determines how many time steps are needed to move the jet forward for one cell. The time step is determined by comparing the lag of the cutting front in the experiments with the lag in the CA model. When the cutting velocity is set in the experiment the time needed for jet to travel 1 mm is determined. Next the lag of the cutting front is measured. The CA model is then set through the coefficient t_c so that the same lag is achieved in simulation. After that the number of time steps needed in simulation for jet to travel 1 mm is determined. If the velocities in experiment and simulation are compared the time step can be calculated by

$$t = \frac{v_s}{v_t}, \tag{9}$$

where t is time step, v_s simulation cutting velocity in mm per iteration and v_t experimental cutting velocity in mms^{-1}.

To be able to simulate kerfing regimes *i.e.* when AWJ does not cut through the workpiece, it is essential to simulate the step on the cutting front, because the step causes significant reduction in the material removal in the lower area of the cut. Because there is no satisfactory explanation when and why the step is formed, it was decided to artificially generate it in the simulation. Two conditions have to be fulfilled in order to start the step formation. First condition is connected to Hashish's (1988) findings, where the connection between the jet width and step formation cycle was established. This was then supported by Guo *et al.*'s (1993) findings about the relation between the striation frequency and the width of the jet, as the step is responsible for forming of the striations. The condition is that the step is generated only when the jet passes the distance of one jet diameter at a preset cutting velocity. The time interval of step generation can be calculated with

$$t_s = \frac{s}{v_t}, \tag{10}$$

where t_s is time interval of step generation and s the jet diameter. The second condition is that there has to be a certain inclination of the cutting front, at the point where the step is formed. With conditions fulfilled, the time and place coordinate of step forming is obtained. At the same time the conditions cause turning off of all cells with AWJ state, which are under the level of the step. By this the similar effect is achieved as when the jet is deflected on the step and the material removal is significantly or completely reduced under the step as it is shown in Figure 4. The step on the cutting front and the jet deflection are marked for better visibility.

4. RESULTS AND DISCUSSION

The presented model was in the first phase compared with experiments performed by AWJ cutting of aluminium alloy AL6061-T6, which is commonly used in AWJ machining research. The lag of the cutting front in CA simulation was indirectly compared with the lag of striations on the surface of the cut. The direct comparison with the cutting front in experiments is not possible because of the opaqueness of the used material. Still the shape of striations can be taken as a good approximation. The measurements of the lag of striations were performed by an optical method, with an example shown in Figure 5, where the least count of the measurement device was 0.01 mm. The experiments were performed on the workpieces with thicknesses of 6 and 15 mm. Cutting was performed at five different cutting velocities for each thickness while the other process parameters stated in Table 1 remained constant during the experiments. The details of experiments and simulation process can be found in the work of Orbanic and Junkar (2004), while in this paper only final results are presented in Figure 6 for the workpiece thickness of 6 mm and in Figure 7 for the workpiece thickness of 15 mm. There can be seen that there is a good match between the experiments and simulation. Figures 6 and 7 (a)–(e) are photographs of the surface cut with striations at different cutting velocities (v_t = 4, 6, 8, 10 and 12 mms^{-1} for 6 mm thickness; v_t = 1, 2, 3, 4 and 5 mms^{-1} for 15 mm thickness). Figures 6 and 7 (f)–(j) are the simulated cutting fronts at different cutting velocities. Different grey scales in these figures represent different states. The black colour represents ES, the white colour represents AWJ and the light grey colour represents MAT.

In the second phase the rules for the step formation were included into the model. The results of non-calibrated simulation for cutting 10 mm thick aluminium with four different cutting velocities are presented in Figure 8. The cutting velocities are represented by the shifting coefficient t_c, where larger number means lower cutting velocity. By using the step formation rules the main achievement was ability to control the depth of cut. In the previous phase the model could simulate only the curvature of the cutting front and could be only used for cutting regimes, where the workpiece is cut through. In Figure 8 it can be seen that if the cutting velocity is increased, the curvature of the cutting front is more distinctive and also the depth of the cut is decreased. It was mentioned in the previous section that the material removal behind the step is significantly reduced. It can be concluded that at larger cutting velocities when the workpiece is not cut through, the step is so large and the step forming cycle is so quick, that the material at the bottom of the cut is not removed at all. This also shows that the workpiece is not cut through only because of the reduced energy of the jet but mainly because of the jet deflection. Often while cutting or kerfing it can be noticed that the jet still has plenty of energy to remove material after it exits the cutting zone.

5. CONCLUSIONS

A two-dimensional CA model for the simulation of AWJ cutting was developed. The model is based on the material removal process, which considers the energy of the AWJ together with its impact angle and erosion resistance of MAT. The rules of CA are designed so that they describe this removal process in combination with the propagation of AWJ intensity. The cutting velocity determines for how long the AWJ will influence a specific part of material. The lower the velocity, the more material is removed and smaller curvature of the cutting front is obtained. The results of CA were compared to striations on the cut surface.

The calibration was performed by matching the lag of the cutting front in the CA with that of the striations in experiments through setting velocity in simulation.

Based on the test data it has been shown that the CA model is able to provide adequate estimation of the shape of the cutting front and the changing of the curvature by changing the cutting velocity. By including step formation rules the model can also simulate cutting in the kerfing regime.

The two-dimensional CA will be in future work expanded into a third dimension in order to obtain other characteristic properties of AWJ cut like taper or surface waviness. The taper of the cut is influenced as in the case of the cutting front by the energy of the jet and the cutting velocity. With the three-dimensional approach some new insights into cutting curved contours and corners will also be obtained.

6. ACKNOWLEDGMENTS

7. REFERENCES

Levy, A. V. "Solid Particle Erosion and Erosion-Corrosion of Materials", Materials Park, OH: ASM International, 1995.

Lebar, A. and Junkar, M.: "Simulation of abrasive water jet cutting process: Part1. Unit event approach. " *Modelling Simul. Mater. Sci. Eng.*, Vol.12, No. 6, pp. 1159-1170, 2004.

Lebar, A. and Junkar, M.: "Simulation of abrasive waterjet machining based on unit event features." *Proc. I. Mech. E., J. Eng. Manuf. – part B*, Vol. 217, No. B5, pp. 699-703, 2003.

Fukunishi, Y., Kobayashi R. and Uchida, K., "Numerical Simulation of Striation Formation on Water Jet Cutting." *Proceedings of 8th American Water Jet Conference*, Vol.2, pp. 657-670, Houston, Texas, 1995.

Sawamura, T., Fukunishi, Y. and Kobayashi R. "Three dimensional model for waterjet cutting simulation." *Proceedings of 9th American Water Jet Conference*, Vol.1, pp. 15-28, Dearborn, Michigan, 1997.

Bitter, J. G. A., "A study of erosion phenomena," Part 1, *Wear*, Vol.6, pp. 5-21, 1963.

Bitter, J. G. A., "A study of erosion phenomena," Part 2, *Wear*, Vol.6, pp. 169-190, 1963.

Vikram G. and Ramesh Babu N., "Modeling and simulation of abrasive water jet cut surface topography." *Proceedings of 11ᵗʰ American Water Jet Conference*, Vol.1, pp. 13-28, Minneapolis, Minnesota, 2001.

Yong, Z., Kovacevic, R. "Modelling of 3D Abrasive Waterjet Machining, part 1 and 2." *Jetting* Technology, Professional Engineering Publishing Limited, Bury St Edmunds, UK, pp. 73-89, 1996.

Ditzinger, T., Friedrich, R., Henning, A., Radons, G. "Non-Linear Dynamics in Modelling of Cutting Edge Geometry." *Proceedings of 10ᵗʰ American Water Jet*, Vol.1, pp. 15-32, Houston, Texas, 1999.

von Neumann, J. "Theory of Self-Reproducing Automata" Urbana, IL: University of Illinois, [Edited and completed by Arthur W. Burks], 1966.

Wolfram, S. "Cellular Automata and Complexity", Reading, MA: Addison-Wesley, 1994.

Chopard, B., Droz, M. "Cellular automata modelling of physical systems", Cambridge University Press, 1998.

D'Ambrosio, D., Di Gregorio, S., Gabriele, S. and Gaudio, R. "A Cellular Automata model for soil erosion by water", *Phys. Chem. Earth (B)*, Vol. 26, pp.33-39, 2001

Karafyllidis, I. and Thanailakis, A. "Simulation of the two-dimensional photoresist etching process in integrated circuit fabrication using cellular automata." *Modeling Simul. Mater. Sci. Eng.*, Vol.3, pp.629-642, 1995.

Karafyllidis, I. "A three-dimensional photoresist etching simulator for TCAD." *Modeling Simul. Mater. Sci. Eng.*, Vol.7, pp.157-168, 1999.

M. Hashish. *Visualisation of the abrasive waterjet cutting process.* Exp. Mechanics, 28, 1988, 159-169.

Guo, N.S., Louis, H. and Meier, G., "Surface structure and kerf geometry in abrasive water jet cutting: formation and optimisation" *Proceedings of 7ᵗʰ American Water Jet*, Vol.1, pp. 1-25, Seattle, Washington, 1993.

Zeng, J. and Kim, T. J. "Machinability of Engineering Materials in Abrasive Water Jet Machining" *Int. J. Water Jet Technology*, Vol.2, pp.103-110, 1995.

Orbanic, H. and Junkar, M.: "Simulation of abrasive water jet cutting process: Part1. Cellular automata approach. " *Modelling Simul. Mater. Sci. Eng.*, Vol.12, No. 6, pp. 1171-1184, 2004.

8. NOMENCLATURE

d	number of dimensions
A	AWJ intensity
M	material removal resistance
N_m	machinability number
R_v	coefficient of material removal in vertical direction
R_h	coefficient of material removal in horizontal direction
i, j	cell coordinates
t	time step
w_1, w_2, w_3, w_4, w_5	weights of the weighted average
S	AWJ source subarray
x	variable
$\lfloor x \rfloor$	floor function
t_c	shifting coefficient
v_s	simulation cutting velocity [mm per second]
v_t	real cutting velocity [mms^{-1}]
t_s	time interval of step generation
s	the jet diameter
p	water pressure [MPa]
$\dot{m}_a$	abrasive mass flow rate [gs^{-1}]
d_o	orifice diameter [mm]
d_f	focusing tube diameter [mm]
h_{so}	stand-off distance [mm]

9. TABLES

Table 1: The process parameters of cutting with AWJ

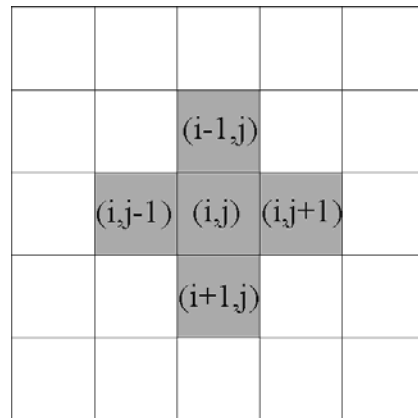| Parameter	Value
p [MPa]	280
$\dot{m}_a$ [gs^{-1}]	5.6
d_o [mm]	0.3
d_f [mm]	0.8
h_{so} [mm]	3
garnet mesh #	80
v_t [mms^{-1}]	4, 6, 8, 10, 12
v_t [mms^{-1}]	1, 2, 3, 4, 5

10. FIGURES

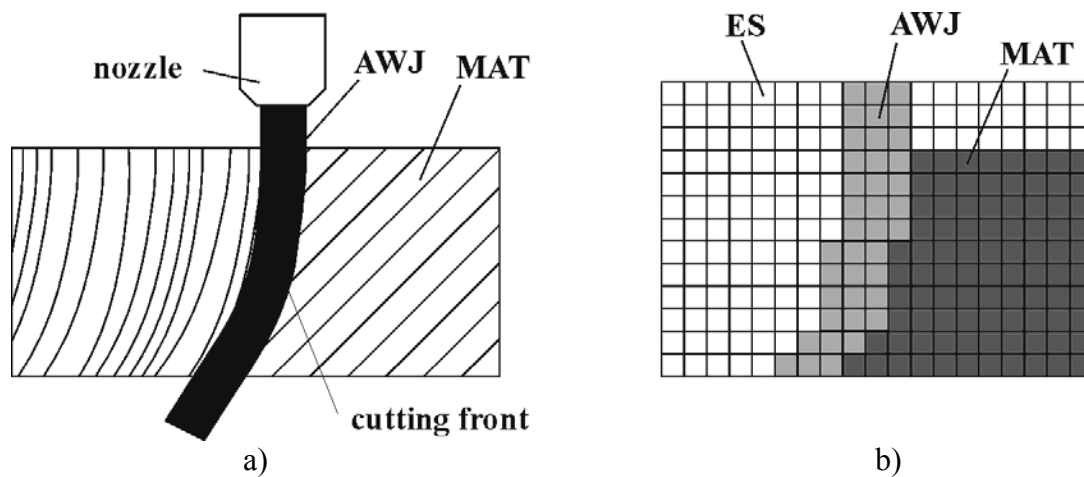**Figure 1:** The von Neumann type of neighbourhood used in the described CA.

Figure 2: The space, where AWJ cutting process takes place, divided into three areas: ES—empty space, AWJ—abrasive water jet and MAT—workpiece material. (*a*) Schematic of a real process. (*b*) Schematic of a simulated process.
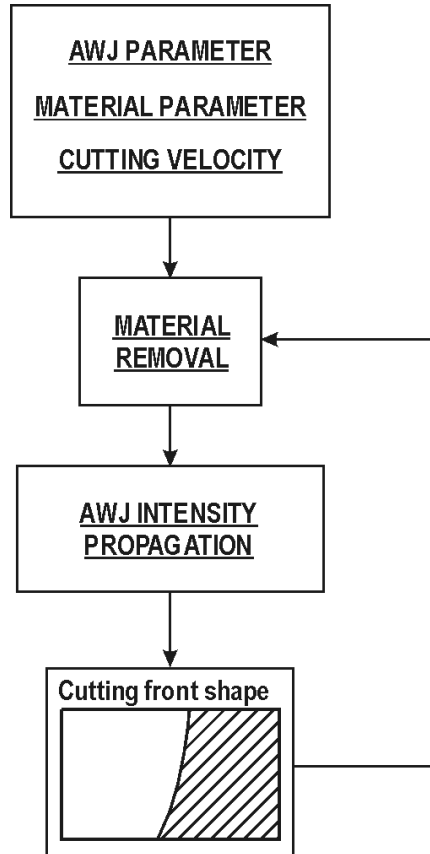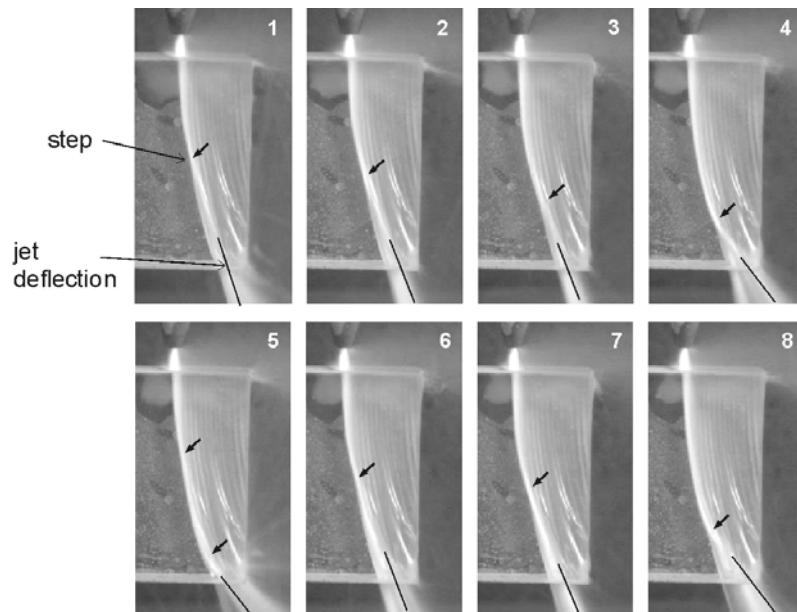
Figure 3: The block diagram of a CA cycle

Figure 4: The step on the cutting front with the jet deflection. The successive figures are numbered sequentially. The time interval between them is 0.04 s.
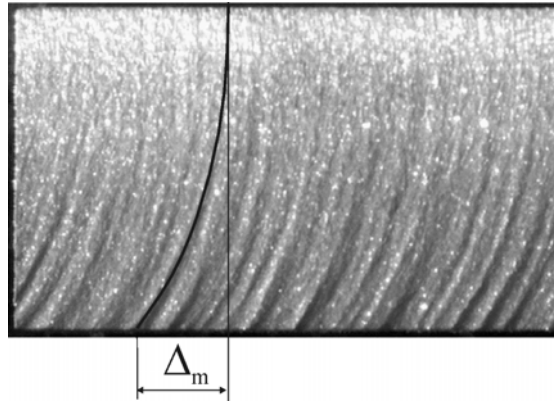
Figure 5: The measurement of the lag of striations on the surface cut by AWJ.
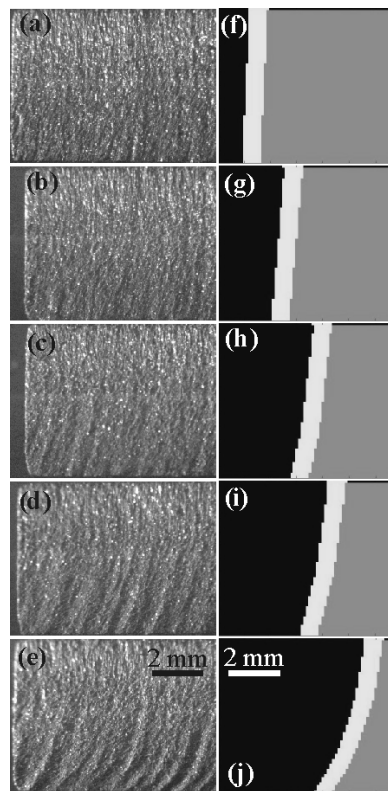

Figure 6: The comparison between striations and the simulation for material thickness of 6 mm. (*a*)–(*e*) Photographs of the cut surface with striations at different cutting velocities (v_t = 4, 6, 8, 10 and 12 mms^{-1}). *(f)–(j)* The simulated cutting fronts at different cutting velocities (Orbanic and Junkar, 2004).
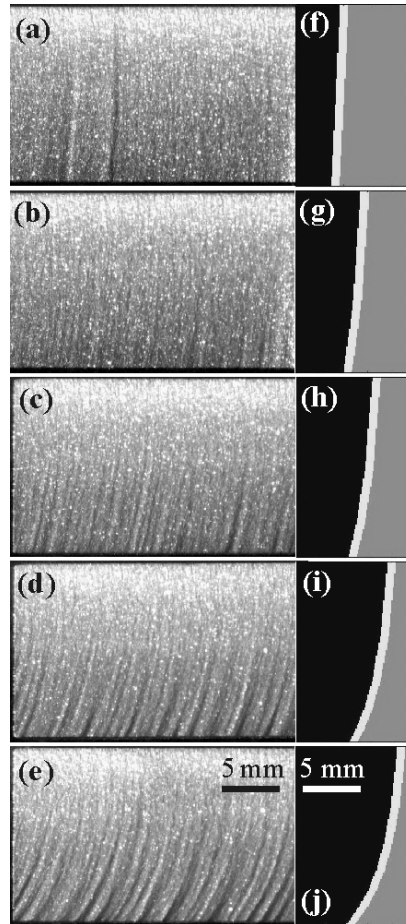
Figure 7: The comparison between striations and the simulation for material thickness of 15 mm. (*a*)–(*e*) Photographs of the cut surface with striations at different cutting velocities ($v_t = 1, 2, 3, 4$ and 5 mms^{-1}). *(f)–(j)* The simulated cutting fronts at different cutting velocities (Orbanic and Junkar, 2004).
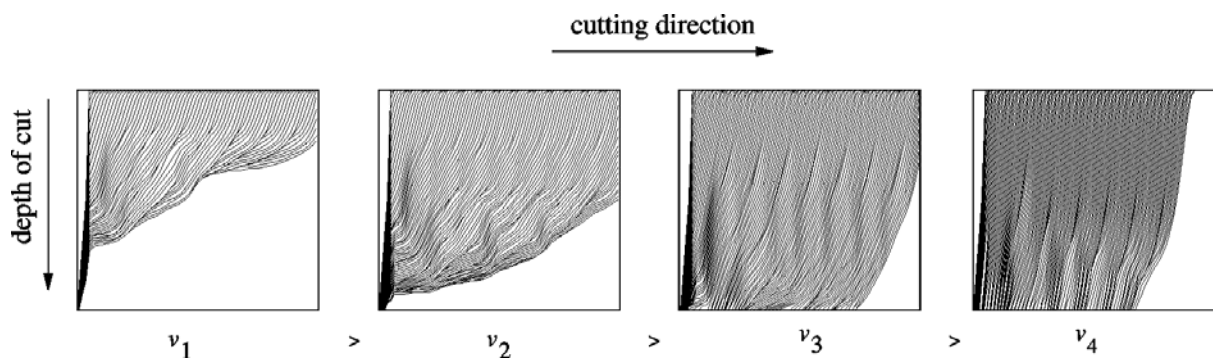

Figure 8: An example of the simulation of cutting with AWJ of a 10 mm thick workpiece of aluminium at different cutting velocities taking into the account the step formation. The cutting velocities are represented by the shifting coefficient t_c, where larger number means lower cutting velocity (tv1=10, tv2)